

# Design of a Multimode Interference-based 1x2 Wavelength-Division-Demultiplexer on an Air-hole Photonic Crystal

Ming-Feng Lu<sup>1,2,\*</sup>, Chung-Yu Hong<sup>1</sup>, Yu-Lin Yang<sup>1</sup>, and Yang-Tung Huang<sup>1</sup>

<sup>1</sup> Institute of Electronics, National Chiao Tung University,  
No. 1001 Da Hsueh Road, Hsinchu, Taiwan, ROC, 300

<sup>2</sup> Department of Electronics Engineering, Ming Hsin University of Science and Technology,  
No. 1 Hsin Hsin Road, Hsinfeng, Hsinchu, Taiwan, ROC, 304  
<http://203.68.227.15/menu/teacher/lmf/index.htm>

*Abstract:* - In this study, the multimode interference (MMI) phenomenon and the self-imaging principle in two-dimensional (2D) photonic crystal (PC) waveguides are investigated. By using the finite-difference time-domain (FDTD) computation, the self-imaging phenomenon and the imaging positions along the propagation path on a PC multimode waveguide are in good agreement with those derived from the modal propagation analysis (MPA). This means that the analytic methods for MMI in conventional multimode waveguides still work in 2D PC waveguides. Moreover, a MMI-based 1-to-2 wavelength-division-demultiplexer is designed on an air-hole photonic crystal structure, which can be applied in a coarse wavelength division multiplexing (CWDM) system. The performance simulated by the FDTD method shows that the insertion loss and the contrast are (0.33 dB, 15.45 dB) and (0.33 dB, 12.9 dB) for the wavelength 1480 nm and 1625 nm, respectively.

*Key-Words:* - coarse wavelength division multiplexing, demultiplexer, imaging length, multimode interference, photonic crystal.

## 1 Introduction

Optoelectronic devices with photonic crystals (PCs) have attracted extensive interest in recent years. Photonic crystals are artificial materials with periodically modulated refractive indices that exhibit photonic band gaps (PBGs). Propagation of light with frequency within the PBGs is forbidden. While introducing line defects into PC structures, PC waveguides are formed and provide a powerful way to manipulate the flow of electromagnetic waves.

Multimode interference (MMI) phenomenon is an observable fact in multimode devices. Based on the self-imaging principle, a field profile can be reproduced in single or multiple images at regular intervals along the path of propagation [1]. MMI effect can be offered in the applications of optical power splitters/combiners, switches, wavelength demultiplexing, and Mach-Zehnder interferometer, etc [2-3]. Those devices are important components for integrated optoelectronic circuits due to the features of MMI, like simple structure, low polarization dependence, low loss, and large optical bandwidth. But in the district of photonic crystals, only a few researchers focus on this topic [4-5]. Power splitters based on the MMI effect in PC waveguides were presented [6]. A wavelength demultiplexer can be realized on a dielectric rod PC structure by the MMI theory [7-8].

The air-hole PC structures can be fabricated on the silicon-on-insulator (SOI) or air-bridge slabs. But the band diagrams of air-hole PC structures are more complicated than those of dielectric rod PC structures, there is still no one discussing the design of wavelength demultiplexer on an air-hole PC structure by the MMI theory. In this study, the theoretical design of a multimode interference-based 1-to-2 wavelength-division-demultiplexer on an air-hole PC structure will be presented. Band diagrams are calculated by the plane wave expansion (PWE) method to get the information of guided modes, and the modal propagation analysis (MPA) used in conventional multimode devices is used to predict the image positions. Then the steady-state field distribution is simulated by the finite-difference time-domain (FDTD) method to have the actual image positions. Comparing the results analyzed by the MPA and FDTD, it is true that the conventional MMI theory still works in PC multimode waveguides. Therefore, we can design a photonic crystal wavelength-division-demultiplexer based on the multimode interference theory, and evaluate its performance.

In the following sections, the MMI effect in a PC multimode waveguide will be investigated. The design of MMI-based wavelength demultiplexers on an air-hole PC structure will also be presented. Finally, its performance will be evaluated.

## 2 Self-imaging Phenomena in PC Multimode Waveguides

The operation of MMI devices is based on the self-imaging principle. In conventional optical waveguides, the guiding mechanism depends on the total internal reflection. The MPA proposed first in [9] is used to predict the image positions in conventional multimode devices. Other approaches make use of ray optics [10], hybrid methods [11], or BPM type simulations. For high index-contrast waveguide, the penetration depth is very small. This leads to a simple dispersion relation.  $L_\pi$  is defined as the beat length of the two modes [1], and

$$L_\pi = \frac{\pi}{\beta_0 - \beta_n}, \quad (1)$$

where  $\beta_n$  is the propagation constant of the  $n$ th mode. While an input field is introduced into the multimode waveguide, the direct single images reproduced at  $2(m+1)(3L_\pi)$ , the mirrored single images reproduced at  $(2m+1)(3L_\pi)$ , and the two-fold images reproduced at  $(2m+1)(3L_\pi)/2$ , where  $m = 0, 1, 2, \dots$ . So we can easily predict the imaging length, and design MMI devices on conventional waveguides.

Because the confinement mechanism in PC waveguides depends on PBG, not total internal reflection, the self-imaging phenomena in PCWs are not the same as in the conventional waveguides. Therefore, the approximated equations and the rules for designing MMI devices in conventional waveguides cannot be directly applied to those cases in PC waveguides. Modal propagation analysis is probably the most theoretical tool to describe the self-imaging phenomena in multimode waveguides. It not only supplies the basis for numerical model, but it also provides insight into the mechanism of multimode interference. Here we use the MPA for the formulation of the periodic imaging in PCs.

Assuming that the input wave is continuous and the spatial spectrum of the input field is narrow enough not to excite the unguided modes, the total input field  $\Psi(y,0)$  at  $z = 0$  in the multimode region can be decomposed into the guided modes and expressed as

$$\Psi(y,0) = \sum_{n=0}^{p-1} c_n \varphi_n(y), \quad (2)$$

where  $\varphi_n(y)$  is the modal field distribution,  $c_n$  is the field excitation coefficient,  $p$  is the number of modes, and the subscript  $n$  denotes the order of the mode ( $n = 0, 1, 2, \dots, p-1$ ). Assuming the time dependence implicit hereafter, the field profile at a distance  $z$  can

then be written as a superposition of all the guided mode field distributions

$$\Psi(y,z) = \sum_{n=0}^{p-1} c_n \varphi_n(y) \exp[j(\beta_0 - \beta_n)z]. \quad (3)$$

The profile of  $\Psi(y,z)$  and the types of images formed will be determined by the modal excitation  $c_n$ , and the properties of the mode phase factor  $\exp[j(\beta_0 - \beta_n)z]$ , where  $\beta_0$  and  $\beta_n$  are the propagation constants of the fundamental mode and the  $n$ th mode. The length  $L_d$  of direct images satisfies

$$(\beta_0 - \beta_n)L_d = 2p_n\pi, \text{ with } p_n = 1, 2, 3, \dots, \quad (4)$$

and we obtain

$$\Psi(y, L_d) = \Psi(y, 0). \quad (5)$$

The length  $L_m$  of mirror images satisfies

$$\begin{aligned} (\beta_0 - \beta_n)L_m &= 2q_n\pi, \text{ for even modes and} \\ (\beta_0 - \beta_n)L_m &= (2q_n - 1)\pi, \text{ for odd modes} \\ &\text{with } q_n = 1, 2, 3, \dots, \end{aligned} \quad (6)$$

and we obtain

$$\Psi(-y, L_m) = \Psi(y, 0). \quad (7)$$

## 3 Design of a MMI-based 1-to-2 Wavelength-Division-Demultiplexer on an air-hole PC Structure

In the following a multimode interference-based 1-to-2 wavelength-division-demultiplexer will be designed on an air-hole PC Structure, which can be applied in a coarse wavelength division multiplexing (CWDM) system. The PWE method is used to get the information of propagated modes, the MPA is used to calculate the self-imaging positions, and the FDTD method is used to confirm the positions and to observe the performance of devices. The 2D PC structure we used is a triangular lattice of air holes on a dielectric substrate with refractive index 3.4. The radius of air holes  $r = 0.32a$ , where  $a$  is the lattice constant of the PC. That results an H-polarization bandgap in the frequency range from 0.215 to 0.298 ( $a/\lambda$ ). H-polarization indicates that the electric field is perpendicular to the normal of the lattice plane, which follows the convention used in a photonic crystal. Figure 1 shows the input portion of the MMI-based wavelength-division-demultiplexer. A single line-defect PC waveguide which is formed by removing one row of air holes along the  $\Gamma$ -K direction in the triangular lattice acts as the access waveguide and four consecutive rows of air holes are removed to form the multimode interference region.

The projected band diagram of the four line-defect PC waveguide calculated by the PWE method is illustrated in Fig. 2. From the dispersion curves it can be found that the multimode region supports four

defect modes at the frequency of  $0.253 (a/\lambda)$ . These modes in the wide defect region lead to the operation of multimode interference. Those parameters about these modes at this frequency, including the propagation constants and the symmetry property of modal field patterns, are all listed in Table 1. It is found that there are well-reproduced direct images for these modes at distances about  $36a$ ,  $72a$ , and  $106a$  in the multimode region. The final length of the MMI region must consider the imaging length of another wavelength. By FDTD simulation, the field distribution confirms the predicted imaging positions and is shown in Fig. 3.

From Fig. 2 it can be found that the four line-defect PC waveguide supports three defect modes at another operating frequency  $0.230 (a/\lambda)$ . The parameters of these modes used to calculate the mirrored image  $L_m$  at the frequency of  $0.230 (a/\lambda)$  are listed in Table 2. It is found that there are mirrored single images for these modes at distances about  $15a$ ,  $45a$ ,  $75a$ , and  $105a$ . By FDTD simulation, the field distribution confirms the predicted position and is shown in Fig. 4. If the final length of the multimode interference region is designed as  $105a$ , we can have a mirror image of  $0.230 (a/\lambda)$  and a direct image of  $0.253 (a/\lambda)$  at the end of the MMI region.

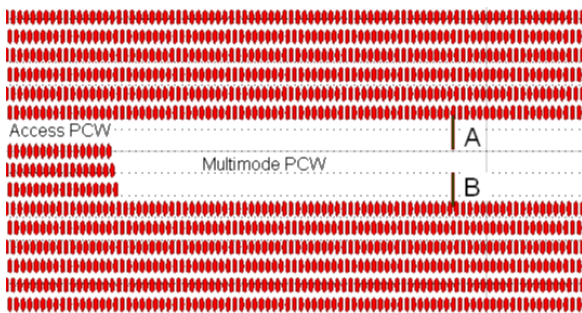


Fig. 1. The input portion of the MMI-based wavelength-division-demultiplexer. A single line-defect PC waveguide acts as the access waveguide

Table 1 Parameters of the four line-defect PC waveguide used to calculate the  $L_d$  at the frequency of  $0.253 (a/\lambda)$ .

number	type	$\beta_n (2\pi/a)$	$\beta_0 - \beta_n$	$2\pi/(\beta_0 - \beta_n)$	$p_n$	$2p_n\pi/(\beta_0 - \beta_n)$	selected $L_d$
0	even	0.149	-	-	-	-	$106a$
1	odd	0.177	0.028	$35.7a$	3	$107a$	$106a$
2	even	0.235	0.084	$11.7a$	9	$105a$	$106a$
3	odd	0.302	0.153	$6.56a$	17	$105a$	$106a$

Table 2 Parameters of the four line-defect PC waveguide used to calculate the  $L_m$  at the frequency of  $0.230 (a/\lambda)$ .

number	type	$\beta_n (2\pi/a)$	$\pi/(\beta_0 - \beta_n)$	$q_n$	even : $\frac{2q_n\pi}{(\beta_n - \beta_0)}$	odd : $\frac{(2q_n - 1)\pi}{(\beta_n - \beta_0)}$	selected $L_m$
0	even	0.228	-	-	-	-	-
1	odd	0.261	$15.0a$	4	-	$105a$	$105a$
2	even	0.313	$5.88a$	9	$106a$	-	$105a$

and four consecutive rows of air holes are removed to form the multimode interference region.

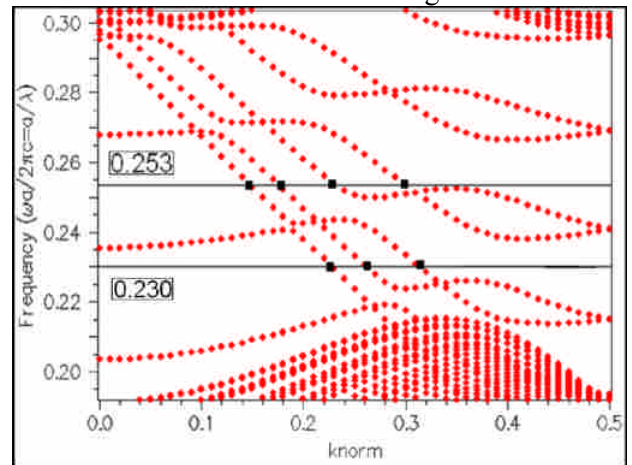


Fig. 2. The projected band diagram of the four line-defect PC waveguide. This multimode PC waveguide supports three guided modes at  $0.230 (a/\lambda)$ , and supports four guided modes at  $0.253 (a/\lambda)$ .

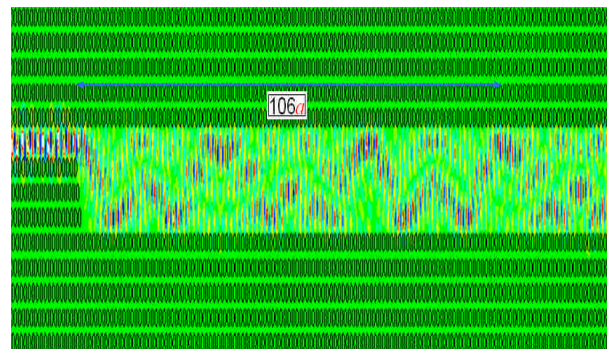


Fig. 3. FDTD simulation results of the steady-state field distribution in the multimode region at  $0.253 (a/\lambda)$ . Direct single images reproduce at the distance about  $36a$ ,  $72a$ , and  $106a$ .

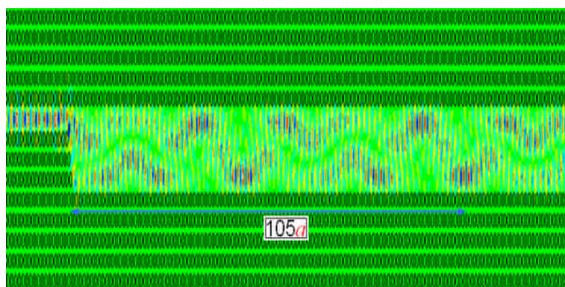


Fig. 4. FDTD simulation results of the steady-state field distribution in the multimode region at 0.230 ( $a/\lambda$ ). Mirrored single images reproduce at the distance about  $15a$ ,  $45a$ ,  $75a$ , and  $105a$ .

Two single line-defect PC waveguides which act as output ports are added to the structure and the whole MMI-based 1-to-2 wavelength-division-demultiplexer is presented in Fig. 5. This device is designed for the usage in a CWDM system. The range of wavelength ( $\lambda$ ) is from 1480 to 1625 nm. Therefore, by setting the lattice constant,  $a$ , as 374 nm, a 1480/1625-nm demultiplexer is constructed. The wave of wavelength 1625 nm is intended to be routed to the output port A, and the wave of wavelength 1480 nm is routed to the output port B. To evaluate the transmission characteristic of this wavelength demultiplexer, two continuous waves with wavelengths 1480 and 1625 nm are launched into the access waveguide. The transmission efficiency is the output power normalized to the input power. The steady-state electric field distributions of the multimode interference-based 1-to-2 wavelength-division-demultiplexer at 1480/1625 nm are shown in Fig. 6. The function of wavelength demultiplexing works well.

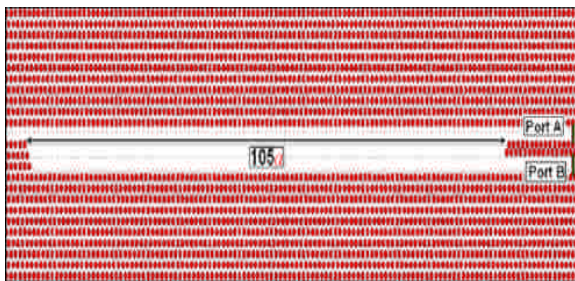
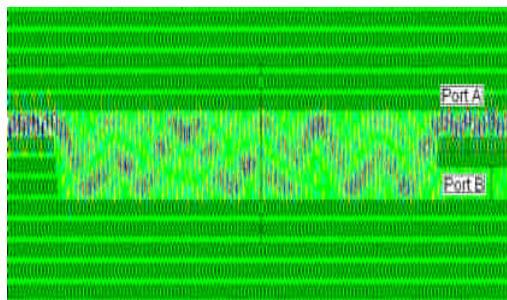
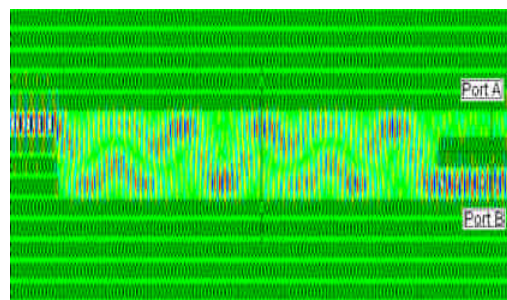


Fig. 5. The multimode interference-based 1-to-2 wavelength-division-demultiplexer designed on an air-hole PC Structure. The length of the multimode interference region is  $105a$ .

Table 3 lists the performance of this device, including two output powers, insertion loss, and contrast. The insertion loss is defined as  $-10 \log(P_{portA(B)} / P_{input})$  and contrast as  $10 \log(P_{portA(B)} / P_{portB(A)})$ ; respectively. The results show that the insertion loss and the contrast are (0.33 dB, 15.45 dB) and (0.33 dB, 12.9 dB) for the wavelength 1480 nm and 1625 nm, respectively.



(a)



(b)

Fig. 6. Steady-state electric field distributions of the designed MMI-based 1-to-2 wavelength-division-demultiplexer at (a) 1625 nm, and (b) 1480 nm .

Table 3 The output power, insertion loss, and contrast for the wavelength 1625 and 1480 nm, respectively.

Frequency( $a/\lambda$ )	Port A	Port B	Insertion Loss	Contrast
0.230	4.72%	92.7%	0.329 (dB)	12.9 (dB)
0.253	92.6%	2.64%	0.334 (dB)	15.5 (dB)

### 4 Conclusion

In our investigation, we have found that the multimode interference still exists in multimode PC waveguides just as in conventional multimode waveguides. The imaging positions calculated by the FDTD simulation have a good agreement to that derived by the MPA method. This means that the analytic methods for MMI in conventional multimode waveguides still can be applied in 2D PC waveguides. Based on the self-imaging principle, a MMI-based 1-to-2 1480/1625-nm wavelength-division-demultiplexer is designed on an air-hole PC

structure. The results show that the insertion loss is about 0.334 dB for the wavelength 1480 nm and 0.329 dB for 1625 nm, respectively. The contrast is about 15.5 dB and 12.9 dB for the wavelength 1480 nm and 1625 nm, respectively. However, there is still much room for further research on the self-imaging phenomena in multimode PC waveguides. For example, a different image length for H-polarization and E-polarization makes it possible to design a MMI-based polarization beam splitter on a PC structure. And the multiple images in multimode PC waveguides lead to the design of 1-to-N power splitters. These devices having substantial size reductions compare with their conventional counterparts. There are still many issues that we should study or improve when designing the MMI devices on a PC. At first, the light line problem must be considered when a full three-dimensional system is established. Another issue is that the image length becomes longer abruptly when the width of multimode PC waveguides is broadened. This is due to their larger dispersion relation in a multimode PC waveguide than in a conventional waveguide, and may cause the device size to increase. It would be a challenge to design a 1-to-N MMI PC device.

## Acknowledgments

The authors would like to thank the National Science Council of the Republic of China under grants NSC 95-2221-E-159-015.

## References:

- [1] L. B. Soldano, and E. C. M. Pennings, "Optical multi-mode interference devices based on self-imaging: principles and applications," *J. Lightwave Technol.*, vol. 13, no. 4, 1995, pp. 615-627.
- [2] M. R. Paiam, C. F. Janz, R. I. MacDonald, and J. N. Broughton, "Compact planar 980/1550-nm wavelength multi/demultiplexer based on multi-mode interference," *IEEE Photonics Technol. Lett.*, vol. 7, no. 10, 1995, pp. 1180-1182.
- [3] Z. Li, Z. Chen, and B. Li, "Optical pulse controlled all-optical logic gates in SiGe/Si multimode interference," *Opt. Express*, vol. 13, no. 3, 2005, pp. 1033-1038.
- [4] Y. Zhang, Z. Li, and B. Li, "Multimode interference effect and self-imaging principle in two-dimensional silicon photonic crystal waveguides for terahertz waves," *Opt. Express*, vol. 14, no. 7, 2006, pp. 2679-2689.
- [5] Z. Li, Y. Zhang, and B. Li, "Terahertz photonic crystal switch in silicon based on self-imaging principle," *Opt. Express*, vol. 14, no. 9, 2006, pp. 3887-3892.
- [6] T. Liu, A. R. Zakharian, M. Fallahi, J. V. Moloney, and M. Mansuripur, "Multimode interference-based photonic crystal waveguide power splitter," *J. Lightwave Technol.*, vol. 22, no. 12, 2004, pp. 2842-2846.
- [7] H. J. Kim, I. Park, B. H. O, S. G. Park, E. H. Lee, and S. G. Lee, "Self-imaging phenomena in multi-mode photonic crystal line-defect waveguides: application to wavelength demultiplexing," *Opt. Express*, vol. 12, no. 23, 2004, pp. 5625-5633.
- [8] Q. Zhu and B. Li, "Photonic crystal waveguide-based Mach-Zehnder demultiplexer," *Applied Optics*, vol. 45, no. 35, 2006, pp. 8870-8273.
- [9] R. Ulrich, "Light-propagation and imaging in planar optical waveguides," *Nouv. Rev. optique.*, vol. 6, no. 5, 1975, pp. 253-262.
- [10] R. Ulrich and G. Ankele, "Self-imaging in homogeneous planar optical waveguides," *Appl. Phys. Lett.*, vol. 27, no. 6, 1975, pp. 337-339.
- [11] D. C. Chang, and E. F. Kuester, "A hybrid method for paraxial beam propagation in multimode optical waveguides," *Trans. Microwave Theory Tech.*, vol. 29, no. 9, 1981, pp. 923-933.